Rapamycin restores BDNF-LTP and the persistence of long-term memory in a model of Down's syndrome

Yuniesky Andrade-Talavera [a,1], Itziar Benito [b,c,d,1], Juan José Casañas [b,c], Antonio Rodríguez-Moreno [a], María Luz Montesinos [b,c,*]

[a] Laboratorio de Neurociencia Celular y Plasticidad, Departamento de Fisiología, Anatomía y Biología Celular, Universidad Pablo de Olavide, E-41013 Sevilla, Spain
[b] Departamento de Fisiología Médica y Biofísica, Universidad de Sevilla, E-41009, Sevilla, Spain
[c] Instituto de Biomedicina de Sevilla, IBIS/Hospital Universitario Virgen del Rocío/CSIC/Universidad de Sevilla, Sevilla, Spain
[d] Servicio de Animalario, Hospital Universitario Virgen Macarena (HUVM), E-41009, Sevilla, Spain

ARTICLE INFO

ABSTRACT

Down's syndrome (DS) is the most prevalent genetic intellectual disability. Memory deficits significantly contribute to the cognitive dysfunction in DS. Previously, we discovered that mTOR-dependent local translation, a pivotal process for some forms of synaptic plasticity, is deregulated in a DS mouse model. Here, we report that these mice exhibit deficits in both synaptic plasticity (i.e., BDNF-long term potentiation) and the persistence of spatial long-term memory. Interestingly, these deficits were fully reversible using rapamycin, a Food and Drug Administration-approved specific mTOR inhibitor; therefore, rapamycin may be a novel pharmacotherapy to improve cognition in DS.

1. Introduction

Trisomy of human chromosome 21 leads to Down's syndrome (DS), the most frequent intellectual disability of genetic origin. Deficits in

spatial long-term memory (LTM) and retrieval of explicit memory are well documented in individuals with DS (Carlesimo et al., 1997; Pennington et al., 2003). These data suggest that both hippocampal and prefrontal dysfunction cooperate to produce cognitive disability.

Memory consolidation (i.e., conversion of short-term memory into LTM) requires the synthesis of new proteins that modify synapses both structurally and functionally. Some of these proteins are locally translated from pre-existent dendritic mRNAs. Thus, local translation is crucial for synaptic plasticity, learning and memory (reviewed by Buffington et al., 2014). We previously reported a deregulation of hippocampal local translation due to Akt–mammalian target of rapamycin (mTOR) hyperactivation in Ts1Cje mice, a DS model (Troca-Marin et al., 2011). This pathway is coupled to postsynaptic receptors, including the tropomyosin-related kinase B (TrkB) receptor, to regulate local translation rates and synaptic plasticity (Tang et al., 2002; Takei et al., 2004). In Ts1Cje mice, mTOR hyperactivation provokes abnormally augmented synaptic local translation due to increased brain-derived neurotrophic factor (BDNF)/pro-BDNF levels (Troca-Marin et al., 2011), suggesting a saturation of the BDNF–TrkB–Akt–mTOR regulatory axis. Indeed, Ts1Cje synapses do not respond to exogenous BDNF (Troca-Marin et al., 2011), which could be relevant for impaired learning and memory in DS (Troca-Marin et al., 2014). Very recently, mTOR hyperactivation

was found in *post-mortem* DS brains (Iyer et al., 2014; Perluigi et al., 2014).

Interestingly, the Food and Drug Administration (FDA)-approved specific mTOR inhibitor rapamycin restores the local translation rates of Ts1Cje (Troca-Marin et al., 2011). This fact raises the possibility that rapamycin could have therapeutic potential for DS intellectual disability. Here, we show that CA3–CA1 BDNF-long term potentiation (BDNF-LTP), an mTOR-dependent form of synaptic plasticity, is lacking in Ts1Cje mice. Moreover, these mice show impaired persistence of spatial LTM. Importantly, rapamycin fully reverses both of these phenotypes.

2. Materials and methods

2.1. Animals

Partially trisomic Ts1Cje mice (Sago et al., 1998) were obtained from Jackson Laboratories and maintained on a mixed genetic background as recommended by backcrossing Ts1Cje males to C57BL/6JOlaHsd × C3H/HeNHsd F1 females. This mating system results in a similar proportion of wild-type (WT) and Ts1Cje animals. Sets of male WT and Ts1Cje littermattes were used in the experiments, that were carried out according to the European Union directive (86/609/EU) for the use of laboratory animals and were approved by the local Ethical Committee.

For the electrophysiological recordings, post-natal day 21–30 male mice were used. For the behavioral experiments, male mice between 2 and 4 months of age were used; furthermore, blind animals homozygous for the retinal degeneration mutation $Pde6b^{rd1}$, which segregates in the Ts1Cje colony (Sago et al., 1998), were not used.

2.2. Reagents

BDNF, cycloheximide, K252a and PD98059 were purchased from Sigma-Aldrich. Rapamycin was acquired from Selleck Chemicals and D-AP5 from Tocris Bioscience. For electrophysiological experiments, BDNF, cycloheximide and D-AP5 were directly dissolved in water; rapamycin, K252a and PD98059 stocks were prepared in DMSO (final concentration of DMSO in the perfusion solution 0.1% v/v). For behavioral experiments, rapamycin was prepared in a vehicle solution (saline buffer containing 4% ethanol, 5% Tween® 80 and 5% polyethylene glycol 400) as previously described (Kwon et al., 2003).

2.3. Electrophysiological recordings

Hippocampal slices were prepared as described elsewhere (Rodriguez-Moreno et al., 1998; Andrade-Talavera et al., 2012). The whole brain, including the two hippocampi, was removed in an ice-cold solution containing the following components (in mM): 124 NaCl, 2.69 KCl, 1.25 KH_2PO_4, 2.0 $MgSO_4$, 1.8 $CaCl_2$, 26 $NaHCO_3$, and 10 glucose (pH 7.3, ~300 mOsm). Next, the brain was positioned on the stage of a vibratome slicer (Leica VT 1000S) and cut coronally to obtain 350 μm-thick transverse hippocampal slices. These slices were kept continuously oxygenated for ≥1 h before use. All of the experiments were carried out at room temperature (22–25 °C). The drugs were bath applied, switching between different perfusion lines at a ratio of 3 ml/min. The experiments performed in the presence of rapamycin, cycloheximide or K252a were carried out in slices treated with these compounds 30 min before BDNF application. In PD98059 experiments the slices were pre-incubated at least 1 h prior baseline recording. Field excitatory postsynaptic potentials (fEPSPs) were recorded in the CA1 region and were evoked at 0.2 Hz stimulation with a monopolar electrode placed on Schaffer collateral afferents in the *stratum radiatum*. The distance between the stimulating and recording electrodes was 200 μm. Extracellular recording electrodes were filled with an external solution. In paired-pulse experiments, two consecutive stimuli separated by 40 ms were applied. The basal synaptic transmission in wild-type, Ts1Cje and rapamycin-treated Ts1Cje slices were studied by a stimulus–

response curve, ranging from 0 to 240 μA with a 20 μA increase per step. The mean of six fEPSPs at each stimulation strength was calculated. The data were filtered at 2 kHz and acquired at 10 kHz.

2.4. Barnes maze test

The protocol used for the Barnes maze test was previously described in detail (Sunyer et al., 2007). Briefly, the mouse was first subjected to an adaptation period in which it was exposed to the stimulus (the air jets produced by three fans surrounding the Barnes platform) and guided to the target box by the experimenter. Next, the mouse was allowed to stay in the box for 2 min. After adaptation, the training phase consisted of 4 trials per day (15-min inter-trial interval) for 4 consecutive days. During each trial, the mouse was exposed to the stimulus and allowed to explore for 3 min. The animal was allowed to remain in the box for 1 min after entering the target hole. If the mouse did not find the target box, it was guided to the target hole by the experimenter. The primary latency (time spent to find the target box) was used to evaluate spatial acquisition (learning of the task).

Two probe trials were performed, including one at 24 h and one at 8 days after the training (Sunyer et al., 2007). During the probe trials, the target hole was closed, and the mouse was allowed to explore for 90 s. The time spent in the target quadrant, the time elapsed before exploring the virtual target box for the first time (primary latency) and the number of primary errors (exploration of wrong hole events before exploring the virtual target box for the first time) were used to assess LTM (24 h probe) and the persistence of LTM (8 day probe).

Visual cues were posted around the Barnes maze platform. To avoid olfactory cues, the maze was systematically cleaned with a surface disinfectant (1% CR36) after each trial and rotated around its axis. An automated tracking system (Smart, Harvard Apparatus) was used to monitor and analyze the animals behavior.

For wild-type or Ts1Cje rapamycin-treated mice, rapamycin (10 mg/kg) was administered by intraperitoneal injection during the 5 days prior to the Barnes maze test (one injection per day). The rapamycin was dissolved at 1 mg/ml in a vehicle solution as previously described (Kwon et al., 2003). A group of Ts1Cje mice were treated with vehicle solution following the same injection scheme. Untreated wild-type and Ts1Cje mice did not receive any kind of treatment or manipulation previous to the training phase.

2.5. Statistics

Data are presented as the mean ± SEM. For electrophysiological experiments, significance was assessed using Student's paired t-test. For statistical comparisons, an averaged and normalized slope of the last 5 min of the time course was taken over 60 min after BDNF application. This slope was represented as the mean value of BDNF-potentiation in each experimental condition. For behavioral experiments, data from the Barnes maze acquisition phase were analyzed using a repeated-measured two-way ANOVA with the Bonferroni post-hoc test. To compare the performance at the 24 h probe and the 8 day probe, data were analyzed using Student's paired t-test. A one-sample t-test was used to assess if the mean values obtained in experiments were significantly different from specified values (target quadrant occupancy different from 25% or scores different from 0). The significance level is indicated using asterisks: $^*P < 0.05$, $^{**}P < 0.01$ and $^{***}P < 0.001$.

3. Results

3.1. CA3–CA1 BDNF-LTP is absent in Ts1Cje mice, and it is restored by rapamycin

Synaptic plasticity deficits were previously reported for Ts1Cje mice, including reduced LTP and increased long-term depression (LTD) in the hippocampal CA1 region (Siarey et al., 2005) and decreased dentate-

gyrus (DG) LTP (Belichenko et al., 2007). However, CA3-CA1 BDNF-LTP, a type of synaptic plasticity that requires local dendritic translation (Kang and Schuman, 1996) and depends on mTOR activation (Tang et al., 2002), has not been investigated in a DS mouse model. We previously demonstrated that mTOR-driven local translation is deregulated in the Ts1Cje hippocampus (Troca-Marin et al., 2011); therefore, we first analyzed BDNF-LTP in these mice.

We found that exogenous BDNF application (20 ng/ml) induced a robust synaptic potentiation at CA3–CA1 synapses in wild-type hippocampal slices ($166 \pm 17\%$ of baseline, $n = 9$), as previously shown by Tang et al. (2002). However, BDNF-potentiation was absent in the Ts1Cje hippocampus ($110 \pm 8\%$ of baseline, $n = 15$) (Fig. 1A, C). As expected (Tang et al., 2002), rapamycin (200 nM) abolished BDNF-LTP in the wild-type hippocampal slices ($109 \pm 10\%$ of baseline, $n = 11$), but it remarkably restored this form of plasticity in the Ts1Cje hippocampus ($194 \pm 23\%$ of baseline, $n = 10$) (Fig. 1B, C). This recovery effect was significantly reduced in the presence of 10 μM cycloheximide (CHX) (CHX: $115 \pm 15\%$ of baseline, $n = 7$ versus control: $216 \pm 24\%$ of baseline, $n = 5$; Fig. 1E, F) demonstrating that, similarly to BDNF-LTP in the wild-type (Kang and Schuman, 1996) (CHX: $109 \pm 8\%$ of baseline, $n = 7$ versus control: $157 \pm 7\%$ of baseline, $n = 4$; Fig. 1D,F), it depends on protein translation. Also similarly to BDNF-LTP in the wild-type (Kang and Schuman, 1995), rapamycin-recovered potentiation in Ts1Cje was prevented in the presence of K252a, an inhibitor of

the tyrosine protein kinase activity of TrkB receptors (K252a: $95 \pm 3\%$ of baseline, $n = 7$ versus control: $211 \pm 26\%$ of baseline, $n = 5$; Fig. 2). These data show that rapamycin-restored BDNF-LTP in Ts1Cje mice requires the activation of TrkB receptors.

It is also known that, in addition to mTOR, BDNF signaling through TrkB receptors activates the Ras–ERK (Extracellular signal-regulated kinase) pathway, which enhances synaptic translational rates and participates in different forms of plasticity (reviewed by Panja and Bramham, 2014). However, it is unknown whether the Ras–ERK pathway plays a role on CA3–CA1 BDNF-LTP.

To gain more insight into the mechanisms of the BDNF-LTP observed in wild-type and rapamycin-treated Ts1Cje animals, we checked a possible contribution of ERK signaling in these experimental groups. We performed experiments in the presence of PD98059, a MEK (MAPK/ERK kinase) specific inhibitor. In wild-type mice slices, BDNF-LTP was almost completely prevented in the presence of 50 μM of PD98059 ($121 \pm 12\%$ of baseline, $n = 6$ versus control: $160 \pm 9\%$ of baseline, $n = 9$; Fig. 3A, B). Ts1Cje hippocampal slices treated with 50 μM of PD98059 did not show potentiation in the presence of 200 nM rapamycin after BDNF application (PD98059: $93 \pm 13\%$ of baseline, $n = 6$ versus control: $178 \pm 18\%$ of baseline, $n = 9$; Fig. 3C, D) demonstrating that, similarly to BDNF-LTP in the wild-type, it involves ERK signaling.

Glutamatergic synapses are known to exhibit mechanistically different types of plasticity, and N-methyl D-aspartate receptors (NMDAR)
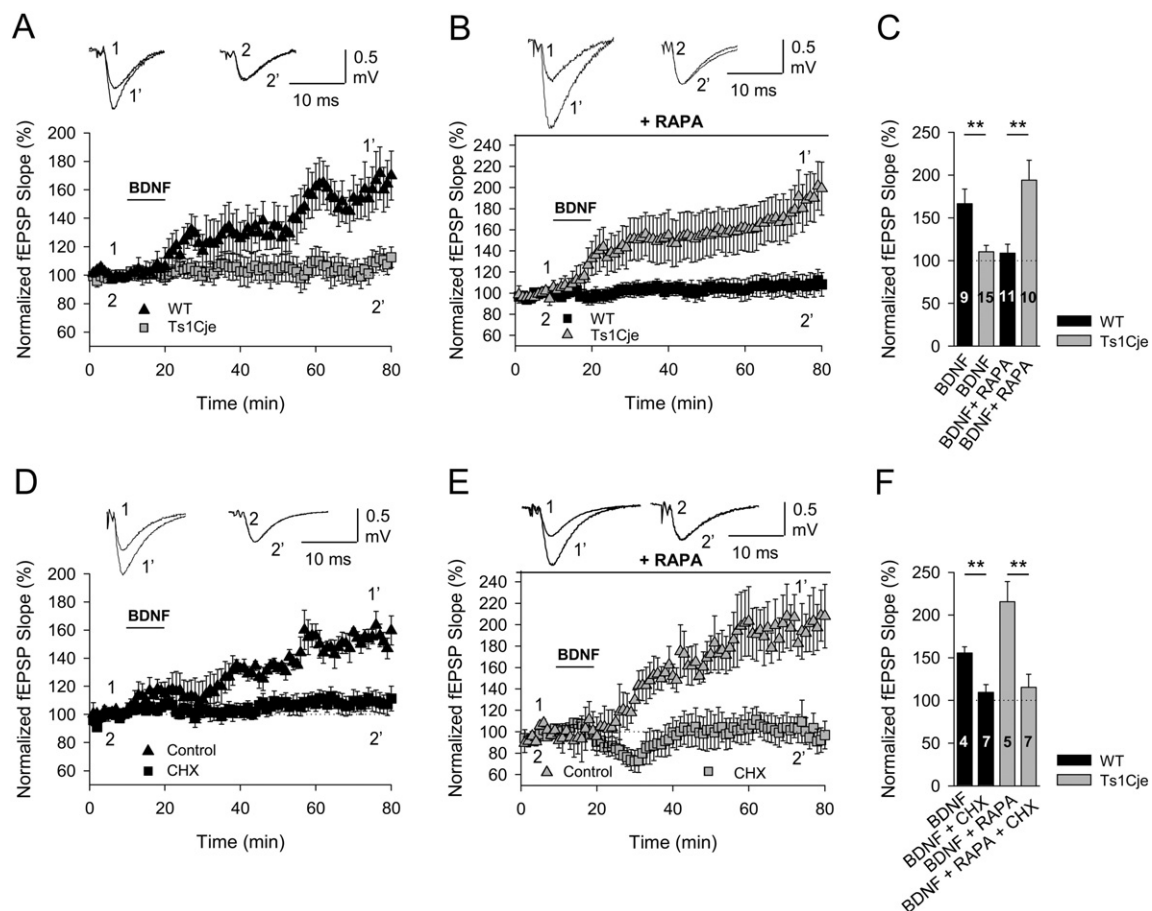
Fig. 1. BDNF-induced LTP at CA3–CA1 hippocampal synapses in WT and Ts1Cje slices treated with or without rapamycin. (A) Time course of BDNF (20 ng/ml) effects on field excitatory postsynaptic potentials (fEPSPs) in WT and Ts1Cje mice. Inset: representative traces of a fEPSP before (1) and after (1′) BDNF application in WT mice and before (2) and after (2′) BDNF application in Ts1Cje mice. (B) Time course of BDNF (20 ng/ml) effects on fEPSPs in slices from WT and Ts1Cje mice treated with rapamycin (200 nM). Inset: representative traces of a fEPSP before (2) and after (2′) BDNF application in WT mice and before (1) and after (1′) BDNF application in Ts1Cje mice. (C) Quantification of the effects depicted in panels A and B. (D) Time course of BDNF (20 ng/ml) effects on fEPSPs in WT slices under control conditions and in slices treated with 10 μM cycloheximide. Inset: representative traces of a fEPSP before (1) and after (1′) BDNF application under control conditions, and before (2) and after (2′) BDNF application in slices treated with 10 μM cycloheximide. (E) Time course of BDNF-induced potentiation in Ts1Cje slices treated with 200 nM rapamycin in control conditions and in the presence of 10 μM cycloheximide. Inset: representative traces of a fEPSP before (1) and after (1′) BDNF application in the absence of 10 μM cycloheximide, and before (2) and after (2′) BDNF application in slices treated with the translation inhibitor. (F) Summary of the results shown in panels D and E. The error bars represent the SEM. The number of slices for each condition is indicated in the corresponding bar. **P < 0.01, Student's t-test.
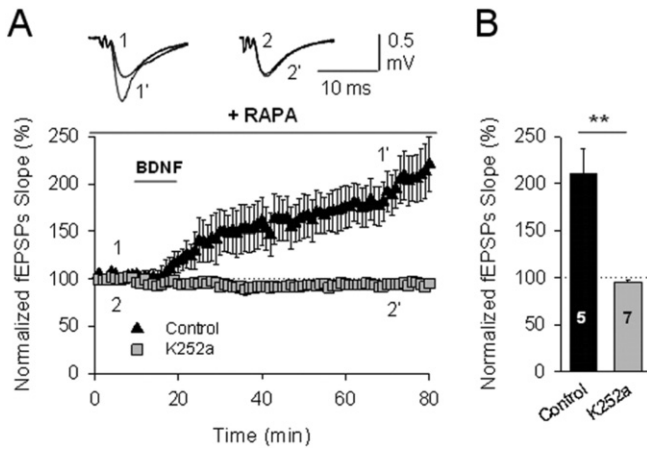
Fig. 2. The effect of the TrkB receptor inhibitor K252a on rapamycin-induced restoration of BDNF-induced LTP at CA3–CA1 hippocampal synapses in Ts1Cje mice. (A) Time course of BDNF-induced potentiation in Ts1Cje slices treated with 200 nM rapamycin in control conditions and in the presence of 200 nM K252a. Inset: representative traces of a fEPSP before (1) and after (1′) BDNF application in the absence of 200 nM K252a, and before (2) and after (2′) BDNF application in slices treated with the TrkB receptor inhibitor. (B) Summary of the results shown in panel A. The error bars represent the SEM. The number of slices for each condition is indicated in the corresponding bar. **$P < 0.01$, Student's t-test.

are widely involved in them. In particular, NMDAR activation can trigger the Ras–ERK pathway (reviewed by Thomas and Huganir, 2004). Thus, we decided to determine whether NMDARs were involved in the rapamycin-restored BDNF-LTP observed in trisomic animals.

In Ts1Cje slices, the rapamycin-recovered BDNF-LTP was not prevented in the presence of the NMDAR antagonist D-AP5 (50 μM D-AP5: $193 \pm 26\%$ of baseline, $n = 4$ versus control: $178 \pm 18\%$ of baseline, $n = 9$; Fig. 3C, D), indicating that NMDARs are not required for this form of LTP. Similar results were obtained in wild-type slices (50 μM D-AP5: $179 \pm 26\%$ of baseline, $n = 5$ versus control: $160 \pm 9\%$ of baseline, $n = 9$; Fig. 3A, B), as previously reported (Kang and Schuman, 1995).

The paired-pulse ratio (PPR) at CA3–CA1 synapses did not change after BDNF application in WT or Ts1Cje slices, regardless of the presence or absence of rapamycin (Fig. 4A, B). These results suggest a postsynaptic mechanism for BDNF-induced potentiation both in WT and rapamycin-treated Ts1Cje slices.

Interestingly, Ts1Cje CA3–CA1 synapses did not show facilitation in response to the paired-pulse protocol (Fig. 4A). Moreover, a clear basal synaptic transmission difference was observed between Ts1Cje and WT mice hippocampal CA3–CA1 synapses (Fig. 4C, D). Remarkably, rapamycin application restored the basal synaptic transmission deficit (Fig. 4C, D) and paired-pulse facilitation (PPF) (Fig. 4B), even in the presence of CHX, K252a or PD98059 (Supplementary Fig. 1), showing that this recovery effect is independent of protein synthesis, TrkB and ERK signaling.

Overall, these experiments are the first to show the impairment of Schaffer collateral-CA1 BDNF-LTP in a DS mouse model. Importantly, we found that the mTOR antagonist rapamycin completely rescues this plasticity deficit. Moreover, rapamycin also restores basal synaptic transmission and short-term plasticity in this DS mouse model.

3.2. The persistence of spatial LTM is impaired in Ts1Cje mice, and it is restored by rapamycin

In addition to its role in hippocampal plasticity (Korte et al., 1995; Kang and Schuman, 1996; Patterson et al., 1996), BDNF is essential for hippocampal-mediated learning and memory (Linnarsson et al., 1997; Mizuno et al., 2000) and for persistence of LTM storage (Bekinschtein et al., 2007). Ts1Cje mice show reduced performance on two hippocampal-dependent memory tests, the Morris maze (Sago et al.,
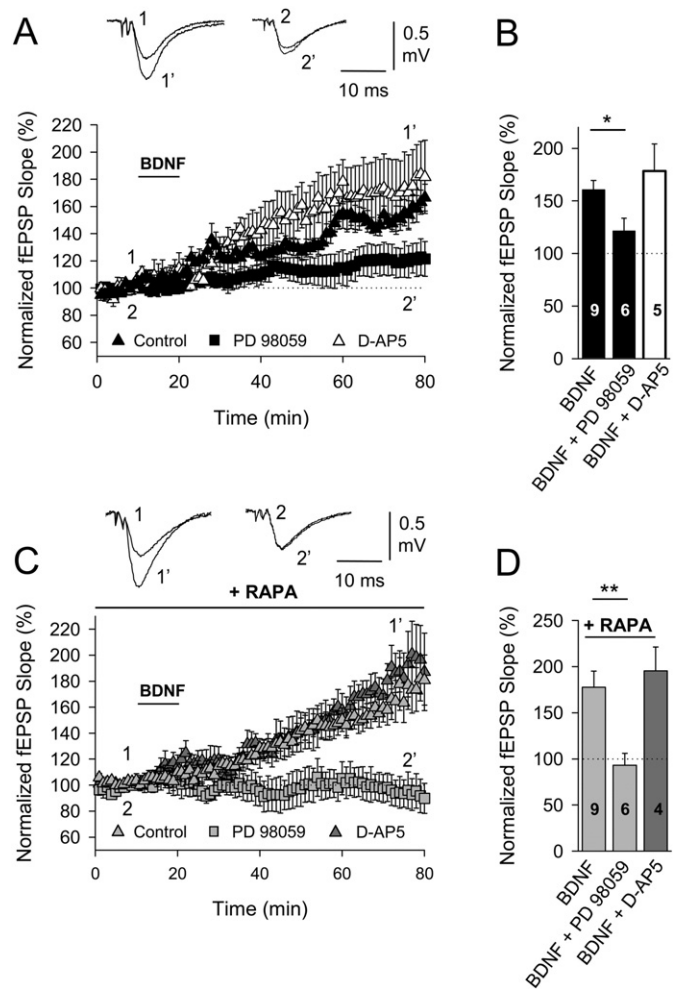

Fig. 3. BDNF-LTP in the CA1 region of the hippocampus involves ERK signaling but not NMDA receptor activation. (A) Time course of the BDNF effect on fEPSP slopes in control conditions (dark triangles), in the presence of 50 μM PD98059 (dark squares) and in the presence of 50 μM D-AP5 (open triangles) in WT mice slices. Inset: representative traces of a fEPSP before (1) and after (1′) BDNF application in the presence of 50 μM D-AP5, and before (2) and after (2′) BDNF application in slices treated with 50 μM PD98059. (B) Summary of results shown in panel A. (C) Time course of the BDNF effect on fEPSP slopes in Ts1Cje slices treated with 200 nM rapamycin in control conditions (gray triangles), in the presence of 50 μM PD98059 (gray squares) and in the presence of 50 μM D-AP5 (dark triangles). Inset: representative traces of a fEPSP before (1) and after (1′) BDNF application in the presence of 50 μM D-AP5, and before (2) and after (2′) BDNF application in slices treated with 50 μM PD98059. (D) Summary of results shown in panel C. The error bars represent the SEM. The number of slices for each condition is indicated in the corresponding bar. * $P < 0.05$, **$P < 0.01$, Student's t-test.

1998) and the T-maze spontaneous alternation task (Belichenko et al., 2007).

Thus, we assessed if rapamycin was able to improve the performance of Ts1Cje mice in a hippocampal-dependent memory test. Given that strong aversive stimuli normally used for reinforcement (such as water in the Morris maze) have been reported to affect animal performance (Hölscher, 1999), we chose the Barnes maze because it is a spatial task similar to the Morris water maze but less stressful for mice (Sunyer et al., 2007). In the Barnes maze, the mouse is placed in a circular, dry platform and is exposed to a weak aversive stimulus (here, a jet air) to induce escape into a target box located under one of 20 holes that are positioned around the perimeter of the platform (Sunyer et al., 2007).

We established four experimental groups: untreated wild-type (WT) and Ts1Cje animals and Ts1Cje mice treated with either vehicle (Ts1Cje vehicle) or 10 mg/kg rapamycin (Ts1Cje RAPA) for the 5 days prior to the training phase (1 intraperitoneal injection per day). We
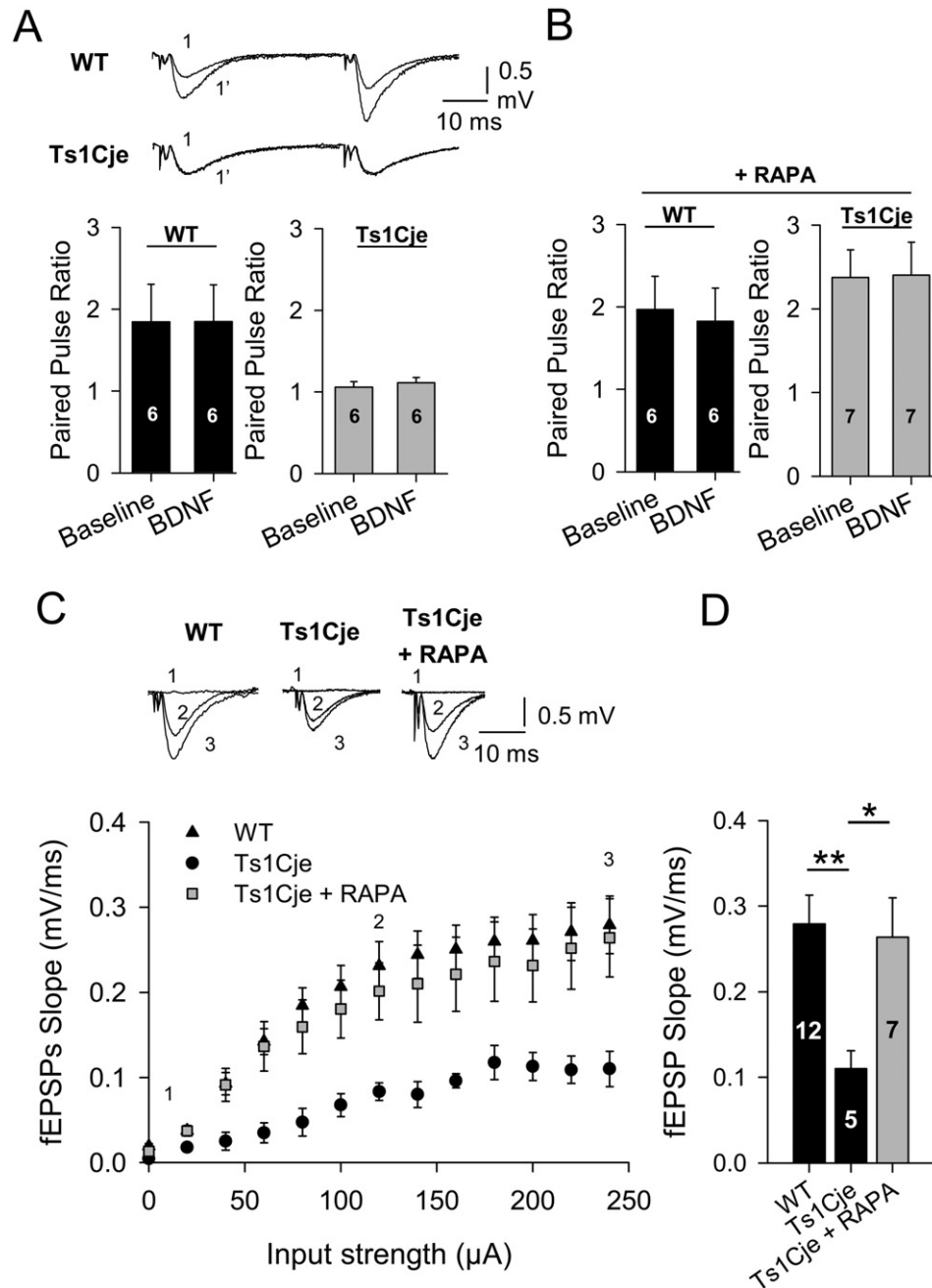
Fig. 4. Rapamycin effect on basal synaptic transmission and paired-pulse ratio (PPR) in Ts1Cje mice. PPR is unaffected by BDNF application in both wild-type and Ts1Cje mice under different experimental conditions. (A) In WT mice, paired-pulse facilitation (PPF) was observed with a 40 ms pulse interval, and it remained unaltered after BDNF application. Thus, the PPR was 1.8 ± 0.5 ($n = 6$) before BDNF treatment (baseline) and 1.8 ± 0.5 ($n = 6$) 60 min after BDNF application. Conversely, there was no facilitation in response to the paired-pulse stimulation protocol in slices from Ts1Cje mice, and similar PPR values were obtained before (baseline: 1.1 ± 0.1; $n = 6$) and after BDNF application (1.1 ± 0.1; $n = 6$). The inset shows representative traces for the PPF protocol in WT and Ts1Cje mice before (1) and after (1′) BDNF application. (B) In the presence of 200 nM rapamycin, PPR at CA3–CA1 synapses before (baseline: 2.1 ± 0.5; $n = 6$) and after BDNF application (1.9 ± 0.5; $n = 6$) did not change in WT mice. The same observation was made in Ts1Cje mice (baseline: 2.5 ± 0.4; $n = 7$; after BDNF: 2.5 ± 0.5; $n = 7$). However, the baseline PPR increased significantly to wild-type levels. (C) Stimulus–strength response curves in WT ($n = 12$), Ts1Cje ($n = 5$) and Ts1Cje slices in the presence of 200 nM rapamycin ($n = 7$). Inset: representative fEPSPs traces. (D) Summary of the results shown in panel C. Note a clear difference in the response curves between WT and Ts1Cje hippocampi. Rapamycin restored this phenotype to the observed in WT slices. The error bars represent the SEM. The number of slices for each condition is indicated in the corresponding bar.*$P < 0.05$; **$P < 0.01$, Student's t-test.

then trained the mice over 4 days (4 trials per day). A significant decrease in primary latency (time spent to find the escape box) over time was observed in all groups ($P < 0.0001$), which demonstrates spatial acquisition (Fig. 5). Although it was not statistically significant, higher mean primary latency values were observed in vehicle-treated Ts1Cje mice on the acquisition phase when compared with untreated Ts1Cje animals (Fig. 5). In addition, when the primary latency values of the 16 given trials were plotted over time, an altered kinetics was

observed in vehicle-treated Ts1Cje mice (Supplementary Fig. 2), suggesting that learning could be slightly affected in these animals.

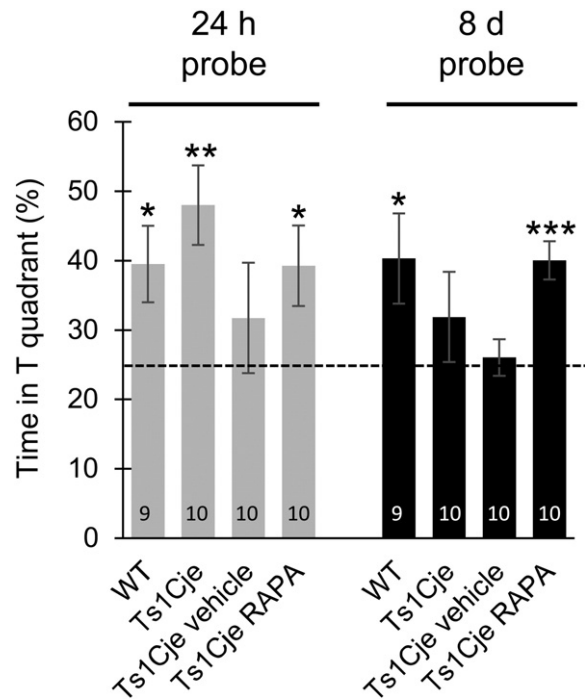Twenty-four hours and 8 days after the training period, the mice were subjected to a probe trial to determine the consolidation and persistence of LTM, respectively (Sunyer et al., 2007). At 24 h, performance was similar among WT, Ts1Cje and Ts1Cje RAPA animals, and the mean time spent in the target quadrant was above chance level (i.e., 25%) in these three groups, which shows that memory was not affected
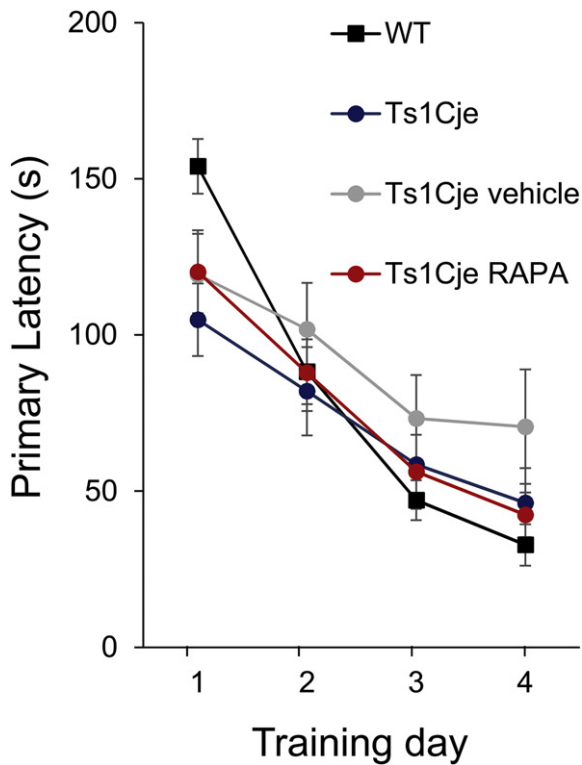
Fig. 5. Spatial learning analysis of untreated wild-type and Ts1Cje animals, and vehicle- or rapamycin-treated Ts1Cje mice. The primary latency (in seconds) to reach the target hole during training days 1 to 4 is represented for untreated wild-type (WT) and Ts1Cje animals and for Ts1Cje mice treated with vehicle (Ts1Cje vehicle) or rapamycin (Ts1Cje RAPA) before the training. The data are expressed as the mean ± SEM of the mean values obtained for each block of 4 daily trials. When the animal was unable to find the target hole in the trial, a maximum primary latency value (i.e., 180 s) was used. A repeated-measured two-way ANOVA with Bonferroni post-hoc tests resulted in $P > 0.05$ values for the comparison of all experimental groups, except for the comparison between WT and Ts1Cje mice at day 1 ($P < 0.05$). However, the same analysis performed to compare non grouped-trials (trial 1 to 16) revealed no significant difference among experimental groups. A significant decrease in primary latency over time was observed in all groups ($P < 0.0001$).

Fig. 6. Analysis of the memory consolidation and memory persistence of untreated wild-type and Ts1Cje animals, and vehicle- or rapamycin-treated Ts1Cje mice. Target quadrant occupancy (expressed as time percentage) during the probe trials given after 24 h and 8 days of (d) Barnes maze training in untreated WT and Ts1Cje mice and in trisomic animals treated with rapamycin (Ts1Cje RAPA) or vehicle (Ts1Cje vehicle). The dashed line indicates the chance level of performance (25%) in the Barnes maze. At 24 h, a one sample t-test for the mean different from 25% showed significant P values in all cases except the Ts1Cje vehicle-treated mice ($P = 0.030$ for WT, $n = 9$; $P = 0.003$ for Ts1Cje, $n = 10$; $P = 0.419$ for Ts1Cje vehicle, $n = 10$; and $P = 0.036$ for Ts1Cje RAPA, $n = 10$). At 8 days, a one sample t-test for the mean different from 25% showed a non-significant P value for only untreated and vehicle-treated Ts1Cje mice ($P = 0.046$ for WT, $n = 9$; $P = 0.318$ for Ts1Cje, $n = 10$; $P = 0.698$ for Ts1Cje vehicle, $n = 10$; and $P = 0.0004$ for Ts1Cje RAPA, $n = 10$). The data are expressed as the mean ± SEM. The number of animals for each condition is indicated in the corresponding bar.

(Fig. 6). However, a lower performance (mean time spent in the target quadrant not statistically different from 25%) was found for Ts1Cje mice treated with vehicle. These data suggest that the vehicle components and/or mice handling prior to the training phase had a negative impact on trisomic mice memory consolidation.

Remarkably, the 8 day probe showed that both untreated and vehicle-treated Ts1Cje mice had reduced exploration of the correct quadrant that was not statistically above the chance level; however, rapamycin-treated Ts1Cje mice exhibited target quadrant exploration times that were similar to WT and above 25% (Fig. 6). An individual comparison of the time spent by each mouse in the target quadrant at 8 days versus 24 h showed a clear reduction in the performance of un-treated Ts1Cje mice at long-term, whereas rapamycin-treated Ts1Cje animals behaved similarly at 24 h and 8 d, and similarly to WT mice (Student's paired t-test for WT 8 days versus WT 24 h, $P = 0.888$, $n = 9$; for Ts1Cje 8 days versus Ts1Cje 24 h, $P = 0.023$, $n = 10$; and for Ts1Cje RAPA 8 days versus Ts1Cje RAPA 24 h, $P = 0.903$, $n = 10$; Fig. 7A). The determination of the "time in T quadrant score", defined as the mean value of the differences between the percentage of time spent in the target quadrant at 8 days and 24 h for each individual, showed a significant negative value for untreated Ts1Cje mice, whereas the WT and Ts1Cje RAPA groups showed values near zero (Fig. 7B). The analysis of other parameters, such as primary latency (Fig. 7C, D) and number of primary errors (Fig. 7E, F), confirmed the reduction of Ts1Cje performance over time and the positive effect of rapamycin. Vehicle-treated Ts1Cje mice performance was similarly affected at

24 h and 8 days in all the analyzed parameters (scores not significantly different from zero; one sample t-test $P = 0.503$, $n = 10$ for "time in T quadrant score"; $P = 0.735$, $n = 10$ for "primary latency score"; $P = 0.755$, $n = 9$ for "primary errors score"; not shown).

Overall, these data demonstrate that although untreated Ts1Cje mice exhibit normal learning and memory consolidation (LTM measured at 24 h) in the Barnes maze, they show significant impairment of LTM persistence. Furthermore, rapamycin completely restores this specific memory phenotype.

4. Discussion

Although synaptic plasticity deficits have been previously reported for Ts1Cje mice (Siarey et al., 2005; Belichenko et al., 2007), here we demonstrated for the first time that CA3-CA1 BDNF-LTP is impaired in a DS mouse model. These findings may shed insight on DS intellectual disability. As mentioned previously, this form of plasticity relies on mTOR-driven local translation (Kang and Schuman, 1996; Tang et al., 2002), a process that is deregulated in Ts1Cje mice due to mTOR hyper-activation (Troca-Marin et al., 2011). Remarkably, mTOR hyperactivation has been recently reported in DS patients (Iyer et al., 2014; Perluigi et al., 2014).

We found that wild-type CA3–CA1 BDNF-LTP also depends on ERK signaling. Activation of TrkB receptors by BDNF is known to activate both the phosphatidylinositol 3-kinase (PI3K)–Akt–mTOR and the Ras–ERK pathways, classically considered as two parallel signaling cascades. However, increasing evidences demonstrate a considerable
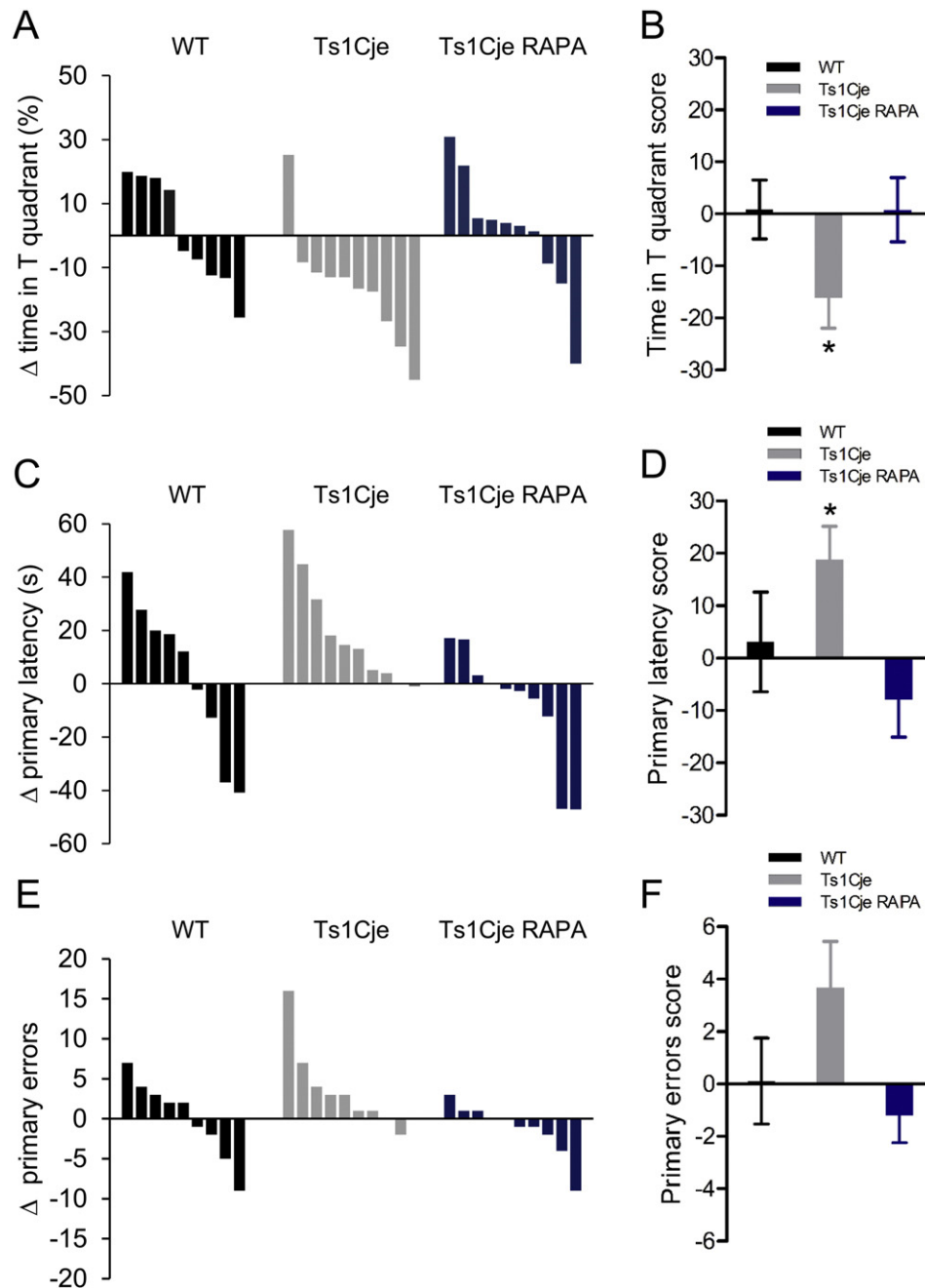
Fig. 7. Differences in target quadrant occupancy, primary latency, and primary errors in the Barnes maze probe trials at 8 days versus 24 h for each individual mouse belonging to the untreated wild-type or Ts1Cje group and to the rapamycin-treated Ts1Cje group. (A) Difference in occupancy of the target quadrant in the 8 day probe versus the 24 h probe (Δ time in T quadrant, expressed as percentage of time) for each untreated WT or Ts1Cje animal and for each rapamycin-treated Ts1Cje (Ts1Cje RAPA) mouse. (B) Time in T quadrant score (mean of the Δ time in T quadrant values showed in panel A) for untreated WT or Ts1Cje and for rapamycin-treated Ts1Cje (Ts1Cje RAPA) mice. A negative score significantly different from zero was only observed in the case of untreated Ts1Cje mice (one sample t-test, $P = 0.888$ for WT, $n = 9$; $P = 0.023$ for Ts1Cje, $n = 10$; $P = 0.903$ for Ts1Cje RAPA, $n = 10$). (C) Difference in primary latency in the 8 day probe versus the 24 h probe (Δ primary latency, expressed in seconds) for each untreated WT or Ts1Cje animal and for each rapamycin-treated Ts1Cje (Ts1Cje RAPA) mouse. (D) Primary latency score (mean of the Δ primary latency values showed in panel C) for untreated WT or Ts1Cje and for rapamycin-treated Ts1Cje (Ts1Cje RAPA) mice. A positive score significantly different from zero was observed only in the case of untreated Ts1Cje mice, indicating that animals belonging to this group took significantly more time to reach the target box at 8 days than 24 h (one sample t-test, $P = 0.756$ for WT, $n = 9$; $P = 0.015$ for Ts1Cje, $n = 10$; $P = 0.292$ for Ts1Cje RAPA, $n = 10$). Maximum primary latency values (i.e., 90 s) were used for one untreated Ts1Cje animal that was unable to find the target box in both probe trials. (E) Difference in the number of primary errors made in the 8 day probe versus the 24 h probe (Δ primary errors) by each untreated WT or Ts1Cje animal and by each rapamycin-treated Ts1Cje (Ts1Cje RAPA) mouse. (F) Primary errors score (mean of the Δ primary errors values shown in panel E) for untreated WT or Ts1Cje animals and for rapamycin-treated Ts1Cje (Ts1Cje RAPA) mice. A positive score that was nearly significantly different from zero was observed only in the case of Ts1Cje mice (one sample t-test, $P = 0.948$ for WT, $n = 9$; $P = 0.071$ for Ts1Cje, $n = 9$; $P = 0.283$ for Ts1Cje RAPA, $n = 10$). The untreated Ts1Cje animal that was unable to find the target box in both probe trials was excluded from this analysis.

cross-talk between both pathways (Fig. 8). Thus, ERK can phosphorylate and activate PDK1 (phosphoinositide-dependent kinase 1) through RSK (p90 ribosomal S6 kinase) (Frödin et al., 2000), which results in activation of the Akt–mTOR pathway in the context of CA1 high frequency stimulation (HFS)–LTP (Tsokas et al., 2007). Moreover, BDNF activates

Calpain-2 through ERK-mediated phosphorylation (Zadran et al., 2010), and it has been recently shown that this event is required for BDNF-induced mTOR activation and dendritic protein synthesis in hippocampus (Briz et al., 2013). Conversely, the PI3K–mTOR pathway is also able to influence ERK activity (Tsokas et al., 2007). The inhibitory
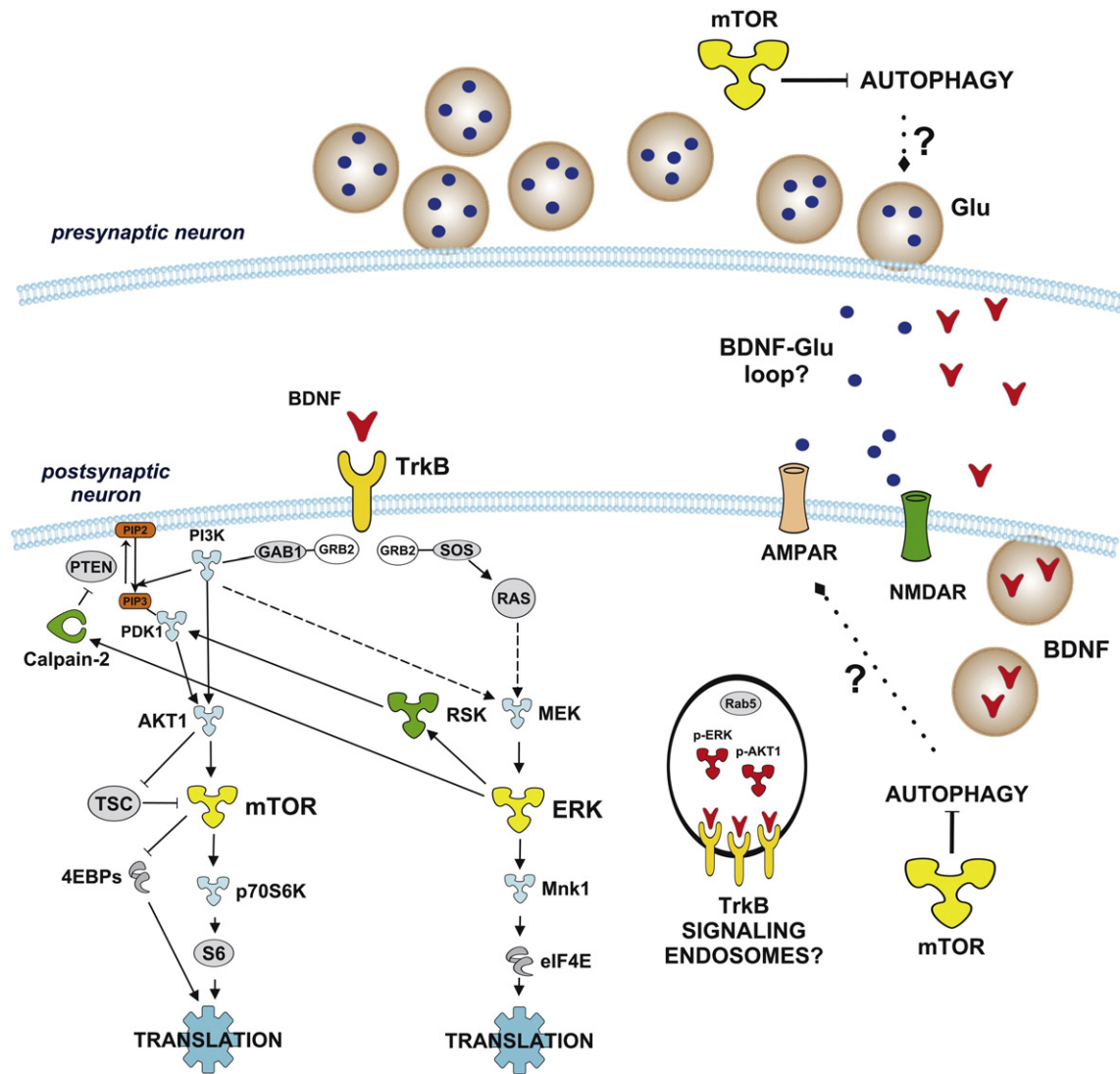
Fig. 8. Synaptic phenotypes of Ts1Cje mice and recovery by rapamycin: a model. Akt–mTOR and Ras–ERK pathways can be triggered by BDNF-activated TrkB receptors to promote local translation of proteins necessary for BDNF-LTP. ERK can indirectly activate mTOR (through RSK or Calpain-2). In WT animals, CA3-CA1 BDNF-LTP depends on mTOR and upstream ERK signaling. In Ts1Cje animals the Akt–mTOR pathway is hyperactivated and does not respond to exogenous BDNF (Troca-Marin et al., 2011). Consequently, BDNF-LTP is absent. Glutamatergic activity through NMDARs is also increased in Ts1Cje hippocampal neurons, and a "BDNF-Glu loop" has been proposed for explaining the synaptic saturation and loss of sensitivity to glutamate and BDNF (Troca-Marin et al., 2014). The mTOR inhibitor rapamycin recovers BDNF-LTP in Ts1Cje, which is elicited by a mechanism that depends on TrkB and ERK, and requires protein synthesis (as is the case in the WT). Rapamycin restores normal local dendritic translation in Ts1Cje hippocampus (Troca-Marin et al., 2011), which could include local translation of BDNF, breaking the saturating BDNF-Glu loop. In this way, the loss of synaptic sensitivity to glutamate (which could explain the Ts1Cje deficits in basal transmission and PPF) and BDNF would be normalized. Consequently, basal transmission, PPF and BDNF-LTP would be restored. Abnormal accumulation of TrkB receptors in signaling endosomes (Nosheny et al., 2015) could also impairs BDNF-LTP in Ts1Cje mice. Autophagy, which is critically controlled by mTOR (and consequently targeted by rapamycin), could also be involved in the PPF and/or basal transmission deficits, by acting on presynaptic neurotransmission (Hernandez et al., 2012) and postsynaptic turnover of glutamate receptors (Shehata et al., 2012).

effect of both rapamycin and PD98059 in wild-type CA3–CA1 BDNF-LTP suggests that ERK signaling acts upstream mTOR, rather than in parallel, in this plasticity.

We found that rapamycin fully restored BDNF-LTP in the Ts1Cje hippocampus. The mechanism underlying this recovery is similar to that of wild-type BDNF-LTP, because it depends on protein synthesis (Fig. 1E, F), TrkB activity (Fig. 2), ERK signaling (Fig. 3C, D) and is likely postsynaptic (Fig. 4B and Supplementary Fig. 1). However, taking into account the complex BDNF–TrkB signaling network (Fig. 8), we cannot exclude the possibility that rapamycin-restored BDNF-LTP in Ts1Cje was exclusively due to a compensatory, enhanced Ras–ERK signaling. In this context, it is relevant to mention that the Ras–ERK pathway is functional in Ts1Cje hippocampus, since BDNF increases the dendritic amount of phosphorylated (Thr197/202) mitogen-activated protein kinase integrating kinase 1 (Mnk1) as well as (Ser209) eukaryotic translation initiation factor 4E (eIF4E) (Troca-Marin et al., 2011).

Interestingly, Ts1Cje CA3–CA1 synapses did not show facilitation in response to the paired-pulse protocol, and basal transmission was clearly impaired. These findings are in contrast with previous work by Siarey et al. (Siarey et al., 2005), who reported no differences in PPF or basal transmission between wild-type and Ts1Cje CA3-CA1 synapses. However, adult (2–3 months-old) mice were used in their study (Siarey et al., 2005). Here, we used juvenile (21–30 days-old) animals. Nevertheless, other possibilities, including genetic background differences, cannot be excluded.

The deficits in BDNF-LTP, PPF and synaptic transmission detected in our study may be a consequence of the "synaptic saturation state" that we previously found in hippocampal Ts1Cje neurons. In these cells, signaling through postsynaptic NMDAR and TrkB receptors appears to be occluded (Alves-Sampaio et al., 2010; Troca-Marin et al., 2011). The TrkB saturation is due to abnormally increased levels of BDNF/pro-BDNF, which results in both Akt–mTOR hyperactivation

and lack of further activation in response to exogenous added BDNF (Troca-Marin et al., 2011). At the pre-synaptic level, BDNF is known to bind TrkB, which enhances glutamate release (Lessmann et al., 1994; Jovanovic et al., 2000). In turn, glutamate can increase the dendritic release of BDNF/pro-BDNF (Tanaka et al., 2008). Disruption of such a "BDNF-Glu loop" (reviewed by Troca-Marin et al., 2014) by rapamycin might explain the recovery of all the Ts1Cje synaptic phenotypes we observed in this work (Fig. 8). Very interestingly, it has been recently reported that cortical synaptosomes from the DS model Ts65Dn also fail to induce further activation of the TrkB signaling pathway when exposed to BDNF (Nosheny et al., 2015). In this model, increased phospho-TrkB, phospho-Akt and phospho-ERK are found to co-localize with Rab5, a marker of early endosomes, in both GABAergic (pre- and post-synaptically) and glutamatergic (post-synaptically) synapses (Nosheny et al., 2015). Enlarged early endosomes and abnormal trafficking of neurotrophins have been reported in Ts65Dn (Cataldo et al., 2003; Cooper et al., 2001). As the authors discuss, the dysregulated TrkB signaling may contribute to synaptic dysfunction in this DS model, in particular by affecting the development of cortical inhibitory circuits and by increasing GABA release (Nosheny et al., 2015), a well established phenotype in DS (Kleschevnikov et al., 2004; Belichenko et al., 2009; Best et al., 2012; Mitra et al., 2012).

Increased and abnormal localization of activated-TrkB receptors in postsynaptic membrane subdomains of CA1 neurons, as described for cortical neurons (Nosheny et al., 2015), might also collaborate to the defective BDNF-LTP in Ts1Cje. However is less clear how rapamycin could restore BDNF-plasticity in such a scenario.

Rapamycin also restored both basal transmission and PPF in Ts1Cje animals. In the case of PPF, this mechanism of action appears to be independent of protein synthesis, TrkB activation and ERK signaling (Supplementary Fig. 1). Although linked to mTOR hyperactivation, the exact nature of this mechanism remains to be elucidated, and other hypothesis besides the "BDNF-Glu loop" could be considered. Of particular interest, mTOR is a key regulator of autophagy (reviewed by Yamamoto and Yue, 2014), and decreased autophagosome formation is observed in DS individuals (Perluigi et al., 2014). Recent data point to a role of autophagy in the regulation of the presynaptic structure and synaptic transmission, perhaps by affecting the turnover of synaptic vesicles (Hernandez et al., 2012). Interestingly, in hippocampal neurons, autophagy is also involved in α-amino-3-hydroxy-5-methyl-4-isoxazolepropionic acid (AMPA) receptor degradation following LTD (Shehata et al., 2012). Thus, Ts1Cje deficits in PPF and basal transmission could be related to the perturbation of the autophagic function due to mTOR dysregulation.

In this work, we also addressed the therapeutic potential of rapamycin for reversing Ts1Cje memory deficits. In contrast to the previous report using the Morris water maze (Sago et al., 1998), Ts1Cje learning was not affected in the Barnes maze. The mating system used by Sago et al. (Ts1Cje males on a CD1 background; Sago et al., 1998) differs from ours; therefore, it is possible that these contrasting findings are due to genetic background, a factor that crucially influences mouse behavior (Holmes et al., 2002). However, as previously mentioned, the Barnes maze test is also less stressful for mice, another strong factor that affects behavior. In fact, vehicle-injected Ts1Cje mice showed a particular behavioral phenotype during the training phase and a lower performance in the 24 h-probe trial when compared with untreated Ts1Cje animals. This finding may be due to higher stress levels in the former group, related to the handling and intraperitoneal injections previous to the training phase. In any case, it is important to stress that, although Sago et al. (Sago et al., 1998) found a statistically significant reduction in the performance of Ts1Cje mice in the Morris water maze when compared with wild-type mice, the trisomic animals also showed a reduction in latency over time during the training phase and spent more than the 25% of the time in the target quadrant in the probe trial, as is the case in our study, demonstrating that the mice retained the capacity to learn the Morris water maze task (Sago et al., 1998), as we show here for the Barnes maze.

In this study, we found that the persistence of LTM (measured as performance in the 8 day probe trial) was impaired in both untreated and vehicle-injected Ts1Cje mice and restored by rapamycin (Fig. 6). Interestingly, the persistence of LTM storage requires hippocampal protein synthesis and a BDNF-dependent phase (Bekinschtein et al., 2007). However, it is important to highlight that the deficits in synaptic plasticity and memory described here for Ts1Cje mice, although relying on mTOR hyperactivation in both cases, are not necessarily interdependent. Although rapamycin completely abolished CA3–CA1 BDNF-LTP in wild-type slices (Tang et al., 2002 and Fig. 1B, C), rapamycin-treated WT mice showed only subtle deficits in the Barnes maze test at 24 h, and a normal performance at 8 days (Supplementary Table 1). Conversely, in spite of completely lacking BDNF-potentiation, the performance of untreated Ts1Cje mice in the Barnes maze 24 h after training was unaffected (Fig. 6), suggesting that LTM in Barnes maze depends on a type of synaptic plasticity different from hippocampal BDNF-LTP. Notably, other plasticity forms are impaired but not completely abolished in Ts1Cje mice (Siarey et al., 2005), and might be sufficient to maintain spatial memory during that relatively short period of time. In particular, as discussed above, the Ras–ERK signaling pathway, which is also under the control of BDNF through TrkB receptors, is not affected in Ts1Cje hippocampus (Troca-Marin et al., 2011). In this context, it is interesting to mention that maintenance of HFS–LTP in the hippocampal DG is rapamycin-insensitive, but depends on TrkB–ERK signaling to the translational machinery (Panja et al., 2009, 2014). Moreover, induction of BDNF-LTP in the DG is also ERK-dependent (Ying et al., 2002). These types of plasticity could be involved in Barnes-maze LTM. Furthermore, the impaired persistence of LTM found both in untreated and vehicle-treated Ts1Cje animals might rely on cortical, rather than hippocampal, mechanisms (Alonso et al., 2005).

Future experiments will further elucidate the signaling pathways and plasticity types involved in these memory phenotypes.

5. Conclusion

In conclusion, rapamycin fully restores basal transmission, PPF, BDNF-dependent plasticity, LTM persistence in Barnes maze (shown here) and local translation rates (Troca-Marin et al., 2011) in Ts1Cje mice. In addition, mTOR hyperactivation has been found in Ts1Cje mice (Troca-Marin et al., 2011) and in DS patients (Iyer et al., 2014; Perluigi et al., 2014). Importantly, rapamycin is already approved for human use. Taking into account all these arguments, rapamycin/rapalogs might represent a therapeutic opportunity for improving cognition in DS, which deserves further future investigation.

Appendix A. Supplementary data

Supplementary data to this article can be found online at http://dx.doi.org/10.1016/j.nbd.2015.09.005.

References

Alonso, M., Bekinschtein, P., Cammarota, M., Vianna, M.R., Izquierdo, I., Medina, J.H., 2005. Endogenous BDNF is required for long-term memory formation in the rat parietal cortex. Learn. Mem. 12, 504–510.

Alves-Sampaio, A., Troca-Marin, J.A., Montesinos, M.L., 2010. NMDA-mediated regulation of DSCAM dendritic local translation is lost in a mouse model of Down's syndrome. J. Neurosci. 30, 13537–13548.

Andrade-Talavera, Y., Duque-Feria, P., Negrete-Diaz, J.V., Sihra, T.S., Flores, G., Rodriguez-Moreno, A., 2012. Presynaptic kainate receptor-mediated facilitation of glutamate release involves Ca_2+ –calmodulin at mossy fiber–CA3 synapses. J. Neurochem. 122, 891–899.

Bekinschtein, P., Cammarota, M., Igaz, L.M., Bevilaqua, L.R., Izquierdo, I., Medina, J.H., 2007. Persistence of long-term memory storage requires a late protein synthesis- and BDNF-dependent phase in the hippocampus. Neuron 53, 261–277.

Belichenko, P.V., Kleschevnikov, A.M., Masliah, E., Wu, C., Takimoto-Kimura, R., Salehi, A., Mobley, W.C., 2009. Excitatory–inhibitory relationship in the fascia dentata in the Ts65Dn mouse model of Down syndrome. J. Comp. Neurol. 512, 453–466.

Belichenko, P.V., Kleschevnikov, A.M., Salehi, A., Epstein, C.J., Mobley, W.C., 2007. Synaptic and cognitive abnormalities in mouse models of Down syndrome: exploring genotype–phenotype relationships. J. Comp. Neurol. 504, 329–345.

Best, T.K., Cramer, N.P., Chakrabarti, L., Haydar, T.F., Galdzicki, Z., 2012. Dysfunctional hippocampal inhibition in the Ts65Dn mouse model of Down syndrome. Exp. Neurol. 233, 749–757.

Briz, V., Hsu, Y.T., Li, Y., Lee, E., Bi, X., Baudry, M., 2013. Calpain-2-mediated PTEN degradation contributes to BDNF-induced stimulation of dendritic protein synthesis. J. Neurosci. 33, 4317–4328.

Buffington, S.A., Huang, W., Costa-Mattioli, M., 2014. Translational control in synaptic plasticity and cognitive dysfunction. Annu. Rev. Neurosci. 37, 17–38.

Carlesimo, G.A., Marotta, L., Vicari, S., 1997. Long-term memory in mental retardation: evidence for a specific impairment in subjects with Down's syndrome. Neuropsychologia 35, 71–79.

Cataldo, A.M., Petanceska, S., Peterhoff, C.M., Terio, N.B., Epstein, C.J., Villar, A., Carlson, E.J., Staufenbiel, M., Nixon, R.A., 2003. App gene dosage modulates endosomal abnormalities of Alzheimer's disease in a segmental trisomy 16 mouse model of Down syndrome. J. Neurosci. 23, 6788–6792.

Cooper, J.D., Salehi, A., Delcroix, J.D., Howe, C.L., Belichenko, P.V., Chua-Couzens, J., Kilbridge, J.F., Carlson, E.J., Epstein, C.J., Mobley, W.C., 2001. Failed retrograde transport of NGF in a mouse model of Down's syndrome: reversal of cholinergic neurodegenerative phenotypes following NGF infusion. Proc. Natl. Acad. Sci. U. S. A. 98, 10439–10444.

Frödin, M., Jensen, C.J., Merienne, K., Gammeltoft, S., 2000. A phosphoserine-regulated docking site in the protein kinase RSK2 that recruits and activates PDK1. EMBO J. 19, 2924–2934.

Hernandez, D., Torres, C.A., Setlik, W., Cebrian, C., Mosharov, E.V., Tang, G., Cheng, H.C., Kholodilov, N., Yarygina, O., Burke, R.E., Gershon, M., Sulzer, D., 2012. Regulation of presynaptic neurotransmission by macroautophagy. Neuron 74, 277–284.

Holmes, A., Wrenn, C.C., Harris, A.P., Thayer, K.E., Crawley, J.N., 2002. Behavioral profiles of inbred strains on novel olfactory, spatial and emotional tests for reference memory in mice. Genes Brain Behav. 1, 55–69.

Hölscher, C., 1999. Stress impairs performance in spatial water maze learning tasks. Behav. Brain Res. 100, 225–235.

Iyer, A.M., van Scheppingen, J., Milenkovic, I., Anink, J.J., Adle-Biassette, H., Kovacs, G.G., Aronica, E., 2014. MTOR hyperactivation in Down syndrome hippocampus appears early during development. J. Neuropathol. Exp. Neurol. 73, 671–683.

Jovanovic, J.N., Czernik, A.J., Fienberg, A.A., Greengard, P., Sihra, T.S., 2000. Synapsins as mediators of BDNF-enhanced neurotransmitter release. Nat. Neurosci. 3, 323–329.

Kang, H., Schuman, E.M., 1995. Long-lasting neurotrophin-induced enhancement of synaptic transmission in the adult hippocampus. Science 267, 1658–1662.

Kang, H., Schuman, E.M., 1996. A requirement for local protein synthesis in neurotrophin-induced hippocampal synaptic plasticity. Science 273, 1402–1406.

Kleschevnikov, A.M., Belichenko, P.V., Villar, A.J., Epstein, C.J., Malenka, R.C., Mobley, W.C., 2004. Hippocampal long-term potentiation suppressed by increased inhibition in the Ts65Dn mouse, a genetic model of Down syndrome. J. Neurosci. 24, 8153–8160.

Korte, M., Carroll, P., Wolf, E., Brem, G., Thoenen, H., Bonhoeffer, T., 1995. Hippocampal long-term potentiation is impaired in mice lacking brain-derived neurotrophic factor. Proc. Natl. Acad. Sci. U. S. A. 92, 8856–8860.

Kwon, C.H., Zhu, X., Zhang, J., Baker, S.J., 2003. mTor is required for hypertrophy of Pten-deficient neuronal soma in vivo. Proc. Natl. Acad. Sci. U. S. A. 100, 12923–12928.

Lessmann, V., Gottmann, K., Heumann, R., 1994. BDNF and NT-4/5 enhance glutamatergic synaptic transmission in cultured hippocampal neurones. Neuroreport 6, 21–25.

Linnarsson, S., Bjorklund, A., Ernfors, P., 1997. Learning deficit in BDNF mutant mice. Eur. J. Neurosci. 9, 2581–2587.

Mitra, A., Blank, M., Madison, D.V., 2012. Developmentally altered inhibition in Ts65Dn, a mouse model of Down syndrome. Brain Res. 1440, 1–8.

Mizuno, M., Yamada, K., Olariu, A., Nawa, H., Nabeshima, T., 2000. Involvement of brain-derived neurotrophic factor in spatial memory formation and maintenance in a radial arm maze test in rats. J. Neurosci. 20, 7116–7121.

Nosheny, R.L., Belichenko, P.V., Busse, B.L., Weissmiller, A.M., Dang, V., Das, D., Fahimi, A., Salehi, A., Smith, S.J., Mobley, W.C., 2015. Increased cortical synaptic activation of TrkB and downstream signaling markers in a mouse model of Down syndrome. Neurobiol. Dis. 77, 173–190.

Panja, D., Bramham, C.R., 2014. BDNF mechanisms in late LTP formation: a synthesis and breakdown. Neuropharmacology 76 (Pt C), 664–676.

Panja, D., Dagyte, G., Bidinosti, M., Wibrand, K., Kristiansen, A.M., Sonenberg, N., Bramham, C.R., 2009. Novel translational control in arc-dependent long term potentiation consolidation in vivo. J. Biol. Chem. 284, 31498–31511.

Panja, D., Kenney, J.W., D'Andrea, L., Zalfa, F., Vedeler, A., Wibrand, K., Fukunaga, R., Bagni, C., Proud, C.G., Bramham, C.R., 2014. Two-stage translational control of dentate gyrus LTP consolidation is mediated by sustained BDNF–TrkB signaling to MNK. Cell Rep. 9, 1430–1445.

Patterson, S.L., Abel, T., Deuel, T.A., Martin, K.C., Rose, J.C., Kandel, E.R., 1996. Recombinant BDNF rescues deficits in basal synaptic transmission and hippocampal LTP in BDNF knockout mice. Neuron 16, 1137–1145.

Pennington, B.F., Moon, J., Edgin, J., Stedron, J., Nadel, L., 2003. The neuropsychology of Down syndrome: evidence for hippocampal dysfunction. Child Dev. 74, 75–93.

Perluigi, M., Pupo, G., Tramutola, A., Cini, C., Coccia, R., Barone, E., Head, E., Butterfield, D.A., Di Domenico, F., 2014. Neuropathological role of PI3K/Akt/mTOR axis in Down syndrome brain. Biochim. Biophys. Acta 1842, 1144–1153.

Rodriguez-Moreno, A., Sistiaga, A., Lerma, J., Sanchez-Prieto, J., 1998. Switch from facilitation to inhibition of excitatory synaptic transmission by group I mGluR desensitization. Neuron 21, 1477–1486.

Sago, H., Carlson, E.J., Smith, D.J., Kilbridge, J., Rubin, E.M., Mobley, W.C., Epstein, C.J., Huang, T.T., 1998. Ts1Cje, a partial trisomy 16 mouse model for Down syndrome, exhibits learning and behavioral abnormalities. Proc. Natl. Acad. Sci. U. S. A. 95, 6256–6261.

Shehata, M., Matsumura, H., Okubo-Suzuki, R., Ohkawa, N., Inokuchi, K., 2012. Neuronal stimulation induces autophagy in hippocampal neurons that is involved in AMPA receptor degradation after chemical long-term depression. J. Neurosci. 32, 10413–10422.

Siarey, R.J., Villar, A.J., Epstein, C.J., Galdzicki, Z., 2005. Abnormal synaptic plasticity in the Ts1Cje segmental trisomy 16 mouse model of Down syndrome. Neuropharmacology 49, 122–128.

Sunyer, B., Patil, S., Höger, H., Lubec, G., 2007. Barnes maze, a useful task to assess spatial reference memory in the mice. Protoc. Exch. http://dx.doi.org/10.1038/nprot.2007.390.

Takei, N., Inamura, N., Kawamura, M., Namba, H., Hara, K., Yonezawa, K., Nawa, H., 2004. Brain-derived neurotrophic factor induces mammalian target of rapamycin-dependent local activation of translation machinery and protein synthesis in neuronal dendrites. J. Neurosci. 24, 9760–9769.

Tanaka, J., Horiike, Y., Matsuzaki, M., Miyazaki, T., Ellis-Davies, G.C., Kasai, H., 2008. Protein synthesis and neurotrophin-dependent structural plasticity of single dendritic spines. Science 319, 1683–1687.

Tang, S.J., Reis, G., Kang, H., Gingras, A.C., Sonenberg, N., Schuman, E.M., 2002. A rapamycin-sensitive signaling pathway contributes to long-term synaptic plasticity in the hippocampus. Proc. Natl. Acad. Sci. U. S. A. 99, 467–472.

Thomas, G.M., Huganir, R.L., 2004. MAPK cascade signalling and synaptic plasticity. Nat. Rev. Neurosci. 5, 173–183.

Troca-Marin, J.A., Alves-Sampaio, A., Montesinos, M.L., 2011. An increase in basal BDNF provokes hyperactivation of the Akt–mammalian target of rapamycin pathway and deregulation of local dendritic translation in a mouse model of Down's syndrome. J. Neurosci. 31, 9445–9455.

Troca-Marin, J.A., Casañas, J.J., Benito, I., Montesinos, M.L., 2014. The Akt–mTOR pathway in Down's syndrome: the potential use of rapamycin/rapalogs for treating cognitive deficits. CNS Neurol. Disord. Drug Targets 13, 34–40.

Tsokas, P., Ma, T., Iyengar, R., Landau, E.M., Blitzer, R.D., 2007. Mitogen-activated protein kinase upregulates the dendritic translation machinery in long-term potentiation by controlling the mammalian target of rapamycin pathway. J. Neurosci. 27, 5885–5894.

Yamamoto, A., Yue, Z., 2014. Autophagy and its normal and pathogenic states in the brain. Annu. Rev. Neurosci. 37, 55–78.

Ying, S.W., Futter, M., Rosenblum, K., Webber, M.J., Hunt, S.P., Bliss, T.V.P., Bramham, C.R., 2002. Brain-derived neurotrophic factor induces long-term potentiation in intact adult hippocampus: requirement for ERK activation coupled to CREB and upregulation of arc synthesis. J. Neurosci. 22, 1532–1540.

Zadran, S., Jourdi, H., Rostamiani, K., Qin, Q., Bi, X., Baudry, M., 2010. Brain-derived neurotrophic factor and epidermal growth factor activate neuronal m-calpain via mitogen-activated protein kinase-dependent phosphorylation. J. Neurosci. 30, 1086–1095.